Mitochondrion 30 (2016) 42–50

Contents lists available at ScienceDirect

Mitochondrion

journal homepage: www.elsevier.com/locate/mito

Uncoupling protein 2 protects mice from aging

Misa Hirose [a], Paul Schilf [a], Falko Lange [b], Johannes Mayer [b], Gesine Reichart [b], Pallab Maity [c], Olaf Jöhren [d], Markus Schwaninger [d], Karin Scharffetter-Kochanek [c], Christian Sina [e], Christian D. Sadik [f], Rüdiger Köhling [b], Bruno Miroux [g], Saleh M. Ibrahim [a,*]

[a] Lübeck Institute of Experimental Dermatology, University of Lübeck, Lübeck, Germany
[b] Oscar-Langendorff-Institute of Physiology, Rostock University Medical Center, Rostock, Germany
[c] Department of Dermatology and Allergic Diseases, University of Ulm, Ulm, Germany
[d] Institute of Experimental and Clinical Pharmacology and Toxicology, University of Lübeck, Lübeck, Germany
[e] Molecular Gastroenterology, University Clinic Schleswig-Holstein, Campus Lübeck, Lübeck, Germany
[f] Department of Dermatology, University of Lübeck, Lübeck, Germany
[g] Institute of Physical and Chemical Biology, UMR 7099, CNRS, University Paris-Diderot, Sorbonne Paris Cités, Paris, France

ARTICLE INFO

Article history:
Received 4 March 2016
Received in revised form 24 June 2016
Accepted 24 June 2016
Available online 27 June 2016

Keywords:
UCP2
Lifespan
Premature aging
Metabolism
Insulin/IGF-1 pathway

ABSTRACT

Uncoupling protein (UCP) 2 is a mitochondrial transporter protein that plays various roles in cellular metabolism, including the glucose and lipid metabolism. Polymorphisms in UCP2 are associated with longevity in humans. In line with this, mice carrying the UCP2 transgene under the control of hypocretin promoter were reported to have an extended lifespan, while, conversely, mice deficient in *Ucp2* demonstrated a significantly shorter lifespan. In this study, we examined the phenotype of aging in a large colony of *Ucp2*-deficient ($Ucp2^{-/-}$) mice on the molecular level. We have found that the significantly shorter lives of $Ucp2^{-/-}$ mice is the result of an accelerated aging process throughout their entire lifespan. Thus, $Ucp2^{-/-}$ mice not only earlier gained sexual maturity, but also earlier progressed into an aging phenotype, reflected by a decrease in body weight, increased neutrophil numbers, and earlier emergence of spontaneous ulcerative dermatitis. Intriguingly, on the molecular level this acceleration in aging predominantly driven by increased levels of circulating IGF-1 in $Ucp2^{-/-}$ mice, hinting at a crosstalk between UCP2 and the classical Insulin/IGF-1 signaling aging pathway.

© 2016 Elsevier B.V. and Mitochondria Research Society. All rights reserved.

1. Introduction

Uncoupling proteins (UCPs) belong to the mitochondrial transporter family and are expressed in the inner membrane of mitochondria (Rousset et al., 2004). While UCP1 expression is restricted to brown adipocytes to produce heat in response to cold stimulation, UCP2 is widely expressed in mammalian tissues and cells, particularly in those of the immune system, including spleen, thymus, leukocytes, macrophages, and bone marrow cells (Fleury et al., 1997). Although UCP2 mRNA has also been found in brain, kidney, lung, heart, skeletal muscle, as well as white and brown adipose tissue (Fleury et al., 1997), UCP2 protein expression has been detected in lung, intestine, immune cells (Emre et al., 2007; Pecqueur et al., 2001), as well as brain (Andrews et al., 2008; Fang et al., 2014). The biochemical and physiological roles of UCP2 are still under debate. Among mitochondrial carrier proteins, *UCP2* has the closest homology to *UCP1* (Fleury et al., 1997), but in contrast to UCP1 it does not contribute to thermogenesis by uncoupling the respiratory chain activity from ATP production. Although a putative mild uncoupling activity of UCP2 is still matter of debate (Bouillaud, 2009; Krauss et al., 2002), several studies have shown that UCP2 contributes to the metabolic regulation of glucose (Vozza et al., 2014) and lipids (Samec et al., 1998; Pecqueur et al., 2008; Moon et al., 2015), most likely by exporting C4 metabolites out of mitochondria (Vozza et al., 2014). For instance, *Ucp2*-deficient cells display a metabolic shift from fatty acid oxidation to glycolysis (Pecqueur et al., 2008). Finally, mice deficient in *Ucp2* demonstrate unique metabolic phenotypes with significantly enhanced serum insulin and lower blood glucose levels (Zhang et al., 2001).

Aging is defined as a process of intrinsic deterioration that is reflected at the population level by an increased likelihood of death and a decline in the production of offspring (Partridge and Gems, 2002). The hallmark of aging is dysfunction in nutrient signaling pathways maintaining metabolic homeostasis (Riera and Dillin, 2015). Therefore, it is quite plausible that *UCP2* may contribute to aging and age-related diseases by modulating metabolism. In fact, polymorphisms in *UCP2* are associated with lifespan in humans (Rose et al., 2011; Barbieri et al., 2012). Rose et al. reported that *UCP2* and *UCP3* SNPs are associated with lifespan, indicating an impact of the SNPs on metabolic rate and oxidative stress, i.e. all minor allele combinations in 2 *UCP2*

* Corresponding author at: Lübeck Institute of Experimental Dermatology, University of Lübeck, Ratzeburger Allee 160, 23538 Lübeck, Germany.
E-mail addresses: Misa.Hirose@uksh.de (M. Hirose), Saleh.Ibrahim@uksh.de (S.M. Ibrahim).

http://dx.doi.org/10.1016/j.mito.2016.06.004
1567-7249/© 2016 Elsevier B.V. and Mitochondria Research Society. All rights reserved.

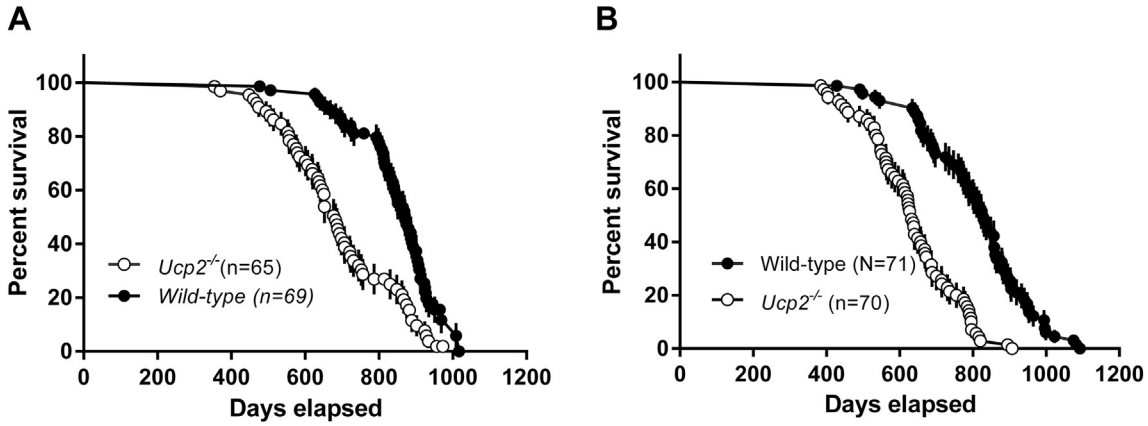

Fig. 1. *Ucp2*$^{-/-}$ demonstrated significantly shorter lifespan compared with wild-type mice. Lifespan of male (A) and female (B) mice. In both sex, mice deficient in the *Ucp2* gene lived significantly shorter than wild-type mice: ***$p < 0.0001$; Log-rank Mantel Cox test.

genes (rs660339 and rs659366) and a *UCP3 gene* (rs15763) were associated with reduced lifespan, while all major allele combinations in the same SNPs were associated with increased lifespan. Barbieri et al. demonstrated that the combination of SNPs in the *IGF1R*, *IRS2* with that in *UCP2* is associated with longevity as a consequence of a better energy metabolic profile. More specifically, all minor allele (A/A in *IGF1R*, Asp/Asp in *IRS2* and Val/Val in *UCP2*) combination was associated with longer longevity. Furthermore, experimental evidence suggested that neuronal-specific overexpression of *UCP2* extended lifespan by reduction of the core body temperature in mice (Conti et al., 2006) and by reduction of oxidative damage in fruit flies (Fridell et al., 2005), although overexpression of *UCP2* did not alter lifespan in mice (Andrews and Horvath, 2009). Moreover, deficiency in *Ucp2* resulted in a significantly shorter lifespan in mice due to increased levels of mitochondrial reactive oxygen species (ROS) in tissue cells (Andrews and Horvath, 2009), thus lending support to the free radical theory of aging. However, growing clinical and experimental evidence negate a beneficial effect of antioxidants on health and lifespan, but instead rather indicate a beneficial effect of mitochondrial ROS on lifespan under stress conditions (Ristow, 2014). This novel concept is called "mitohormesis" (Tapia, 2006; Schulz et al., 2007). Considering the increasing evidence that UCP2 plays a major role in cellular metabolism, we sought for additional aging pathways possibly involved in the shorter lifespan phenotype and the age-related physiological/pathological alterations in a large cohort of mice deficient in *Ucp2*.

2. Materials and methods

2.1. Mice and husbandry

Ucp2$^{-/-}$ (B6·129S4-Ucp2^{tm1Lowl}/J, stock number; 005934) and *C57BL/6J* wild-type (stock number; 000664) mice were obtained from Jackson laboratory (Bar Harbor, ME, USA). Mice were provided ad libitum access to filtered water and autoclaved pellet diet (Altromin, Eastern-Westphalia/Lippe, Germany). The animal facility was maintained at 21 °C on a 12 h light-12 h dark cycle. Mice were allocated into two study groups: longitudinal study group to evaluate lifespan, and cross sectional study group to evaluate the mice at different ages.

Animal use was approved by local authorities of the Animal Care and Use Committee (V242-7224.122-5, Kiel, Germany) and performed by certified personnel.

2.2. Longitudinal study

Sixty-four mice per group were calculated using G*Power (Faul et al., 2007) to allow detecting a 10% difference in lifespan with a *p*-value of 0.05 and a power of 0.8. Therefore, 70 male wild-type mice, 71 female wild-type mice, 65 male *Ucp2*$^{-/-}$ mice and 70 female *Ucp2*$^{-/-}$ mice were assigned to the longitudinal study. None of the mice had mating experience. One male wild-type mouse was excluded from the study due to laboratory error. Mice were daily inspected by experienced animal facility staff, and if any unusual observation, including diseases and behavioral changes, was made, it was reported to a veterinarian. All findings were recorded.

Of mice in the longitudinal study, 5 to 6 mice per sex per strain were selected and bled when 3, 6, 12, 18, and 24 months old. Obtained blood cells were tested by flow cytometry to characterize immune cell subpopulations.

2.3. Determining age at death (lifespan)

As previously described, mice were daily inspected. Following slightly modified established clinical criteria (Yuan et al., 2009), a mouse was determined as moribund when demonstrating more than one of the following clinical signs: inability to eat or drink; abnormally low body temperature, severe lethargy (reluctance to move when gently prodded with forceps), severe balance or gait disturbance; rapid weight loss; an ulcerated or bleeding tumor; enlarged abdomen; panting, severe ulcerative dermatitis which covers >20% of body surface. The age, at which a moribund mouse was killed, was taken as the best available estimate of

Table 1
Lifespan analysis in *Ucp2*$^{-/-}$ and wild-type mice.

Sex	Strain	N	Medien survival (days)	Medien decrease (%)	95% CI	Log-rank *p*-value (*p*)	90% percentile age	90% percentile decrease (%)	Age of		Mean age	SEM
									25% death	75% death		
Male	Wild-type	69	869	24.86	809.4–863	<0.0001	965	7.34	795.5	912	836.2	13.44
	Ucp2$^{-/-}$	65	653		645.6–718.7		894.2		577.5	800.5	682.1	18.30
Female	Wild-type	71	828	23.67	775.1–843.3	<0.0001	995.6	20.06	693	903	809.2	17.11
	Ucp2$^{-/-}$	70	632		605.4–663.9		795.9		548	718.8	634.6	14.67

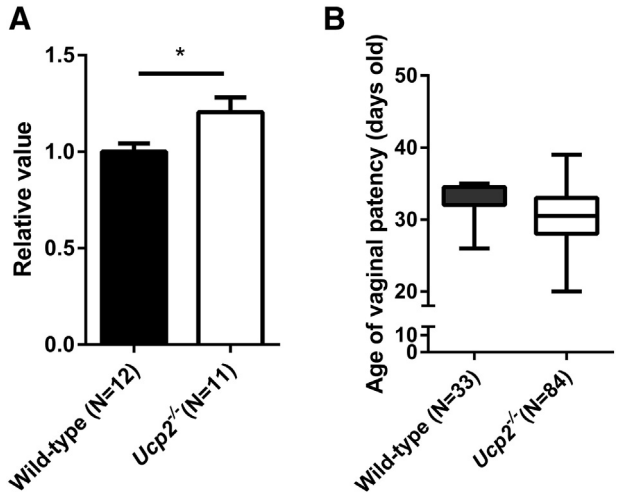

Fig. 2. Higher plasma IGF-1 levels in $Ucp2^{-/-}$ mice and earlier sexual maturity in female $Ucp2^{-/-}$ mice. A. Plasma IGF-1 levels in 6 months old mice (N = 12; wild-type, N = 11; $Ucp2^{-/-}$ mice) were measured using commercially available ELISA. Significantly increased levels of plasma IGF-1 levels were observed in $Ucp2^{-/-}$ mice compared with wild-type mice. Two independent tests with 4–7 samples/strain. The values were normalized to those of wild-type mice in each test: $^{*}p = 0.0178$; *t*-test. B. Vaginal patency was evaluated in female mice. Female $Ucp2^{-/-}$ mice reached sexual maturation earlier than wild-type mice: $^{**}p < 0.01$; *t*-test. All values are presented as mean ± SEM.

its natural lifespan. Moribund mice were autopsied by a veterinarian and clinical and macroscopic observations were recorded. Blood samples were stored at −20 °C, and organ samples were stored in 4% PFA.

2.4. Body weight measurement

At 3, 6, 12, 18 and 24 months, body weight measurement was recorded from mice in both longitudinal and cross sectional study groups.

2.5. Evaluation of peripheral blood cell subpopulation by flow cytometry and complete blood count

Approximately 200 μl peripheral blood was collected from the facial vein of each mouse using an animal lancet in a tube containing EDTA as anticoagulant and prepared as previously described (Petkova et al., 2008). Three different antibody mixtures were prepared and used to dissect comprehensive phenotyping of a series of immune cell population as previously described (Petkova et al., 2008). In brief, mixture 1 was used to stain B cell and with anti-B220 (clone RA3-6B2) antibody. Mixture 2 was used to stain T cell subsets and included: anti-CD8 (clone 53–6.7) FITC, anti-CD62L (clone MEL-14) PE, anti-CD4 (clone RM4–5) PerCP-Cy5.5-eFluor710, and anti-CD44 (clone IM.7) APC-eFluor660. Mixture 3 was used to stain NK, NKT and activated T cell populations and included: Rat anti-mouse NKp46 (clone 29A1.4) FITC, alpha-GalCer:CD1d (clone L363) PE and rat anti-CD4 (clone RM4-5) APC. Antibodies in the study were purchased from eBioSciences (Frankfurt, Germany) and BioLegend (Fell, Germany).

Stained cells were run on the FACS Calibur (BD Bioscience, Heidelberg, Germany) and 10,000 events were acquired per sample. Acquired sample files were analyzed with FlowJo software (Tree Star, Ashland, OR). Gating strategy was followed to the one described previously (Petkova et al., 2008) and the available protocol in Jackson Laboratory Mouse Phenome Database (Grubb et al., 2014).

Complete blood count was analyzed using EDTA-anti-coagulated mouse blood samples on Hemavet 950 (Drew Scientific Inc., FL, USA).

2.6. Blood chemistry

For determining plasma IGF-1 levels, mice were fasted for 4 h (8:00 AM to 12:00 PM) before blood collection. Plasma IGF-1 levels were measured by a commercially available ELISA kit (Mouse/Rat IGF-1 Quantikine ELISA Kit, R&D Systems, Wiesbaden-Nordenstadt, Germany).

2.7. Female sexual maturity

Vaginal patency was observed as previously described (Yuan et al., 2012).

2.8. Indirect calorimetric cage analysis

O_2 consumption, CO_2 production, food/water intake, and locomotor activity were continuously monitored using an open-circuit indirect calorimetry system (PhenoMaster System™, TSE, Bad Homburg, Germany). Mice were allocated to the experimental room system 4 days before measurements to let them acclimatize and then monitored for 5 days. The average values of records taken during last 3 days were used for the analysis. The respiratory exchange ratio (RER) was estimated as ratio of CO_2 produced (ml/h) to O_2 consumed (ml/h). Energy expenditure (EE) was calculated as following: $(3.941 + 1.106 \times \text{RER}) \times O_2$ consumed and normalized to body weight (Weir, 1949).

2.9. Mitochondrial superoxide measurement in brain tissue

Living brain slices (hippocampal horizontal slices; 400 μm) were prepared and mitochondrial superoxide levels were assessed in the slices, as previously described (Mayer et al., 2015). In brief, living brain slices were incubated in artificial cerebrospinal fluid (aCSF) with 1 μM MitoSOX Red (Life Technologies, Darmstadt, Germany) for 15 min at room temperature in dark, followed by washing with aCSF, fixed in 3.7% paraformaldehyde, cryo-protected with 30% sucrose in PBS and frozen at −80 °C. After cutting into 10 μm thick slices, samples were counterstained and mounted with ProLong Gold Antifade Reagent containing 4-,6-diamidino-2-phenylindole (DAPI, Life Technologies). Quantification of ROS levels relative to nucleic area stained with DAPI were performed using confocal laser scanning microscopy (Fluoview FV10i, Olympus, Hamburg, Germany). Five slices of each mouse (n = 5/strain) in each age group (3, 6, 12 and 24 months old) were analyzed and two pictures from three different regions were taken: cornu ammonis area 1 (CA1), cornu ammonis area 3 (CA3) and dentate gyrus (DG).

2.10. Statistical analysis

GraphPad Prism 5 was used for the statistical analysis. Statistical analysis for the lifespan study was performed using log-rank test.

Table 2
Incidence of ulcerative dermatitis. Total of 141 wild-type mice (70 males/71 females) and 137 $Ucp2^{-/-}$ (65 females and 70 females) were evaluated for the onset of ulcerative dermatitis. More $Ucp2^{-/-}$ mice developed the disease compared with wild-type mice ($p = 0.0047$, Fisher's exact test) and showed significantly higher risk of the disease (relative risk; 1.173, 95% CI; 1.048–1.313, odds ratio; 2.528, 95% CI; 1.317–4.851). This suggests the *Ucp2* gene is protective for the age-related skin disease.

Strain	Cases (N)	Cases (%)	Unaffected (N)	Unaffected (%)	Total (N)	*p*-Value	Relative risk	95% CI	Odds ratio	95% CI
Wild-type	16	11.35	125	88.65	141	0.0047	1.173	1.048–1.313	2.528	1.317–4.851
$Ucp2^{-/-}$	33	24.09	104	75.91	137					

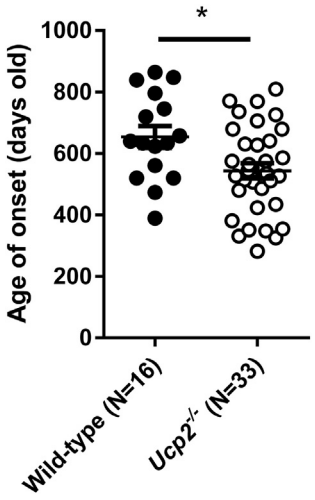

Fig. 3. Earlier onset and higher incidence of ulcerative dermatitis in $Ucp2^{-/-}$ mice. Aged mice developed ulcerative dermatitis. The age of disease onset is shown. $Ucp2^{-/-}$ mice developed the disease significantly earlier than wild-type mice: $^{*}p = 0.0151$; *t*-test.

Fisher's exact test was used to evaluate the incidence of ulcerative dermatitis. Results for all other assays were analyzed using two-way ANOVA or *t*-test. *p*-Values of <0.05 were considered as a statistically significant difference.

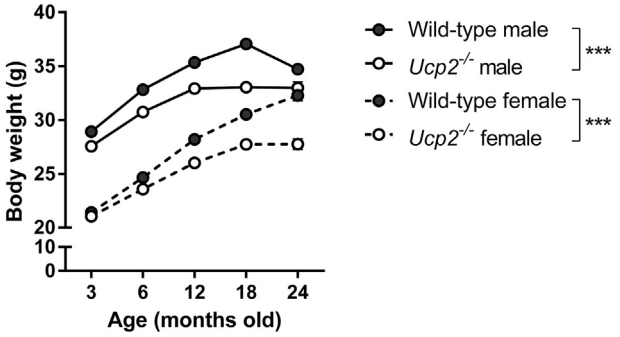

Fig. 5. Significantly reduced body weight throughout the life time in $Ucp2^{-/-}$ mice. $^{***}p < 0.0001$ (two-way ANOVA). All values are presented as mean ± SEM.

3. Results

3.1. The lifespan of Ucp2 $^{-/-}$ mice is significantly shorter than wild-type mice

A total of 140 wild-type ($Ucp2^{+/+}$) mice (69 males and 71 females) and 135 $Ucp2^{-/-}$ mice (65 males and 70 females) were included in the lifespan analysis. The dataset consisted of mice that died of natural causes or were sacrificed when moribund. The survival curves for each sex are presented in Fig. 1.

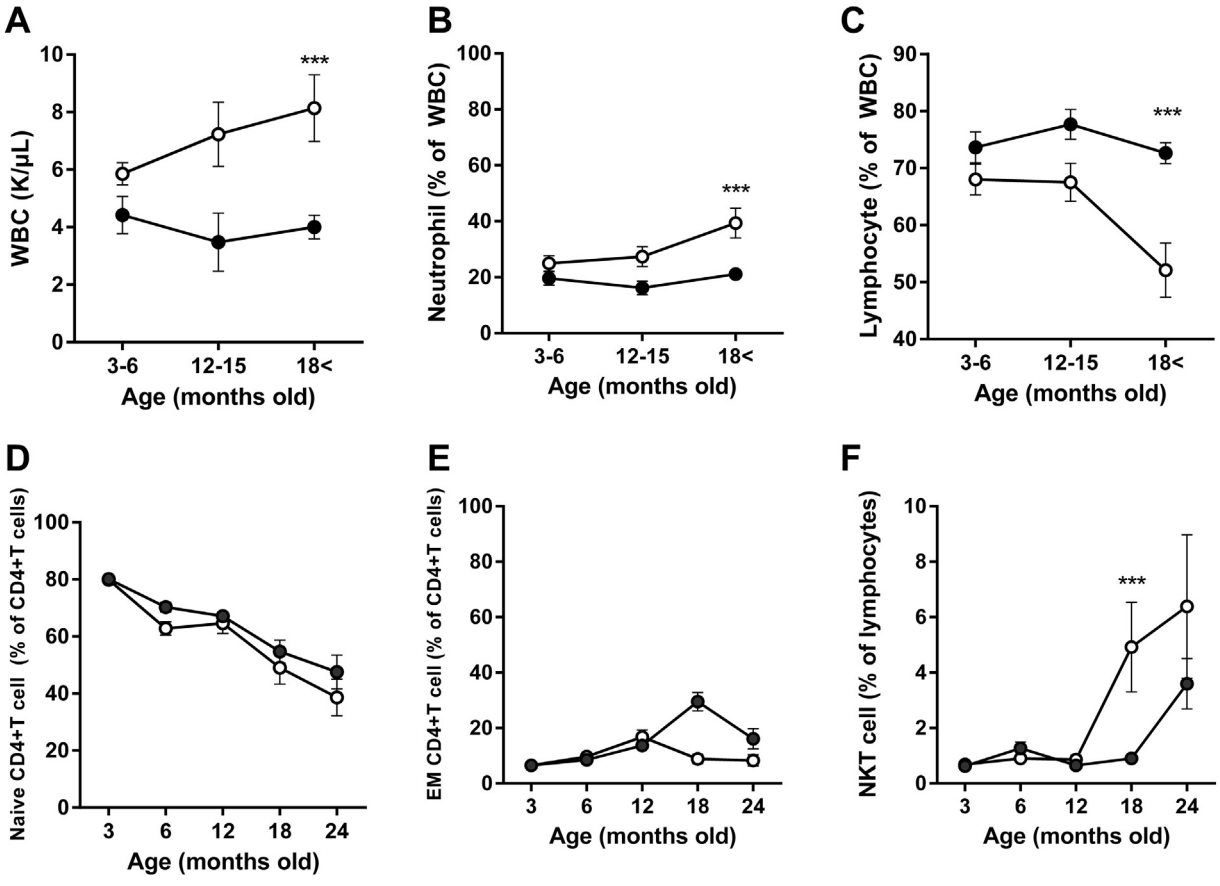

Fig. 4. Immune cell subpopulations in the peripheral blood in $Ucp2^{-/-}$ and wild-type mice at different ages. Peripheral blood was measured by complete blood count (A–C) and flow cytometry (D–E) at different ages. (A) White blood cell count. Number of WBC in $Ucp2^{-/-}$ mice at 18 < month old significantly increased compared to that in age-matched wild-type mice. $p < 0.001$ (two-way ANOVA). (B) Neutrophils. Both $Ucp2^{-/-}$ and wild-type mice demonstrated increased levels of neutrophils in aging: $p < 0.0001$; two-way ANOVA. The neutrophil ratio in $Ucp2^{-/-}$ mice at 18 months significantly higher than that in age-matched wild-type mice: $p < 0.001$; two-way ANOVA. (C) Lymphocyte. Age affects the levels of lymphocytes in both groups: $p < 0.0001$; two-way ANOVA. The percentage of lymphocyte in $Ucp2^{-/-}$ mice demonstrated significant reduction at 18 months of age. (D) Naive CD4+ T cells, (E) effector memory (EM) CD4+ T cells (F) NKT cells: $^{*}p < 0.05$, $^{***}p < 0.001$; two-way ANOVA. For the blood cell count, samples obtained from 18 mice/strain (3–6 months old), 7 mice/strain (12–15 months old) and 16–17 mice/strain (18 < months old) were used. For flow cytometry, blood samples obtained from 11 to 12 mice/strain (3, 6, 12 and 18 months old) and 5–10 mice/strain (24 months old) were tested. White circles indicate $Ucp2^{-/-}$ mice and black ones are wild-type mice. All values are presented as mean ± SEM.

In both males and females, the median lifespan in *Ucp2*$^{-/-}$ mice was significantly decreased by 216 days in males (from 869 to 653 days) and 196 days in females (from 828 to 632 days), or 24.86% in males and 23.67% in females relative to that of wild-type mice ($p < 0.0001$, Log-rank test, Table 1).

3.2. Circulating serum IGF-1 levels are significantly increased in Ucp2-deficient mice, and their sexual maturation is accelerated

Circulating IGF-1 levels in 6 months old mice are correlated with their lifespan (Yuan et al., 2012). To evaluate whether this association

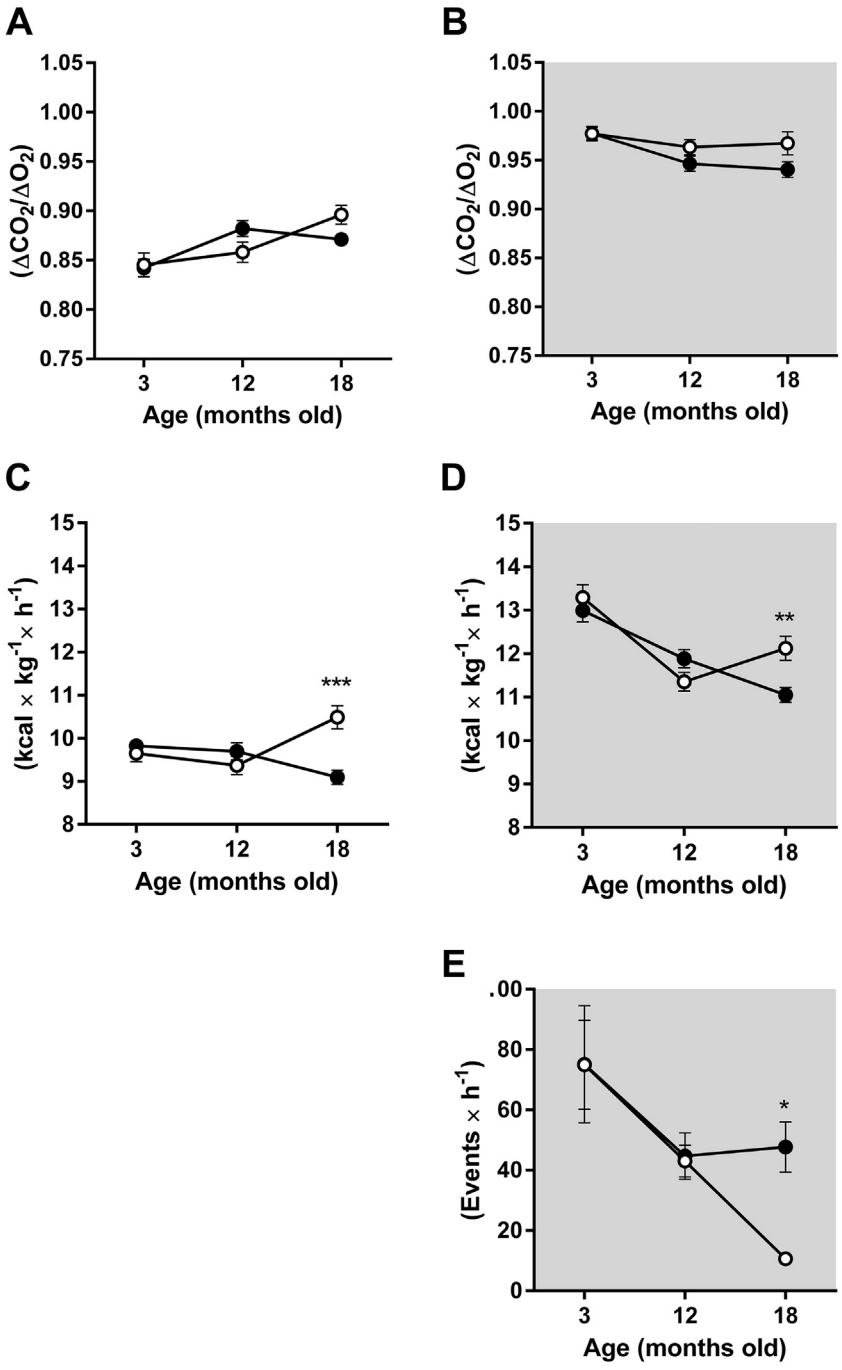

Fig. 6. High use of glucose as energy source and more energy expenditure in aged *Ucp2*$^{-/-}$ mice. Mice were acclimatized 4 days before start of calorimetric assay. Values shown in the figures were the mean of those from day 3 to day 5. Five mice (3 and 12 months old) and 6 mice (18 months old) were used for this assay. A. Respiratory exchange ratio (RER) during the resting period, i.e., day time; from 6:00 to 18:00. Age significantly affected RER in wild-type and *Ucp2*$^{-/-}$ mice: $p < 0.0001$, respectively; two-way ANOVA. B. RER during the active period, i.e., night time; from 18:00 to 5:00. *Ucp2*$^{-/-}$ mice demonstrated significantly higher RER compared with wild-type mice: $p = 0.0492$; two-way ANOVA. There was a significant age impact on RER in wild-type: $p < 0.0001$; two-way ANOVA. C. Energy expenditure (EE) during the resting period. There was a significant interaction between EE and age in wild-type and *Ucp2*$^{-/-}$ mice: $p < 0.01$ and $p < 0.0001$, respectively; two-way ANOVA. At 18 months of age, EE in *Ucp2*$^{-/-}$ was significantly higher than that in wild-type: $p < 0.0001$; two-way ANOVA. D. EE during the active period. In both wild-type and *Ucp2*$^{-/-}$ mice EE was significantly affected by age: $p < 0.0001$, respectively; two-way ANOVA. *Ucp2*$^{-/-}$ mice showed significantly higher EE than wild-type mice at 18 months: $p < 0.0001$; two-way ANOVA. E. Voluntary exercise during the active period. There was a significant age impact on the voluntary exercise in both wild-type and *Ucp2*$^{-/-}$ mice: $p < 0.0001$, respectively; two-way ANOVA. Eighteen months old *Ucp2*$^{-/-}$ mice demonstrated significantly reduced activity compared to wild-type mice: $p < 0.05$; two-way ANOVA. White circles indicate *Ucp2*$^{-/-}$ mice and black ones show wild-type mice. All values are presented as mean ± SEM.

is found in *Ucp2*$^{-/-}$ mice, IGF-1 levels in the plasma of 6 months old mice were determined. IGF-1 levels in *Ucp2*$^{-/-}$ mice were significantly higher than those in wild-type mice (Fig. 2A, mean values normalized to those in wild-type ± SEM: 1.000 ± 0.042 in wild-type; 1.205 ± 0.075 in *Ucp2*$^{-/-}$ mice, $p = 0.0178$, *t*-test).

In addition, IGF-1 levels have been correlated with sexual maturity in females evaluated by vaginal patency, and sexual maturity in females has been highlighted as one of the best predictors of lifespan (Yuan et al., 2012). In line with the higher IGF-1 levels, *Ucp2*$^{-/-}$ mice demonstrated earlier vaginal patency (at 30.18 ± 0.37 days old) than wild-type mice (32.18 ± 0.44 days old; $p = 0.027$, *t*-test).

3.3. Age-associated skin disease is aggravated in *Ucp2*$^{-/-}$ mice

A total of 141 wild-type (70 males and 71 females) and 137 *Ucp2*$^{-/-}$ mice (65 males and 70 females) was examined for the onset of ulcerative dermatitis (UD). UD is common in B6-background mouse strains starting around the age of 12 months and is recognized as age-associated disease (Kastenmayer et al., 2006; Williams et al., 2012). *Ucp2*$^{-/-}$ mice developed UD more frequently ($p = 0.0047$, Fisher's exact test, Table 2) and at a significantly earlier age than wild-type mice (mean age (days old) of UD onset ± SEM: 653.8 ± 35.22 in wild-type; 543 ± 25.22 in *Ucp2*$^{-/-}$ mice, $p = 0.0151$, *t*-test, Fig. 3). This indicates that *Ucp2* exerts physiological functions in maintaining skin homeostasis and protects from age-associated skin disease.

3.4. Accelerated immune senescence in Ucp2-deficient mice

Immune cell subset frequencies in the peripheral blood of wild-type and *Ucp2*$^{-/-}$ mice were assessed by complete blood counts and flow cytometry. The blood count analysis revealed significantly elevated total numbers of white blood cell in over 18 months old *Ucp2*$^{-/-}$ mice in comparison to age-matched wild-type mice (Fig. 4A). Leukocyte differential blood count further showed that specifically the levels of neutrophils were significantly increased in *Ucp2*$^{-/-}$ mice (Fig. 4B) and monocytes (Supplementary Fig. 1A), while, in contrast, the number of lymphocytes was significantly decreased (Fig. 4C). There were no significant differences in the blood counts of eosinophilic granulocytes or basophilic granulocytes between the two strains (Supplementary Fig. 1B, C).

The lymphocyte subpopulation was further characterized by flow cytometry using a panel of immune surface markers. In both strains, the levels of B cells and CD4+ T cells decreased ($p = 0.0327$ and $p < 0.0001$, respectively; two-way ANOVA), and those of CD8+ T cell increased with age ($p = 0.0002$, two-way ANOVA). Despite the aging phenotype, these levels were the same in age-matched *Ucp2*$^{-/-}$ and wild-type mice. In both *Ucp2*$^{-/-}$ and wild-type mice, naive CD4+ T cell (Fig. 4D) and naive CD8+ T cell populations (Supplementary Fig. 2) were significantly decreased in aging ($p < 0.0001$ and $p < 0.0001$, respectively; two-way ANOVA). Memory (i.e., effector memory; EM and central memory; CM) CD4+ and CD8+ T cell populations displayed a trend towards increased numbers in both strains in aging (Fig. 4E and Supplementary Fig. 2). Likewise, NKT cell numbers increased in aging ($p < 0.0001$, two- way ANOVA), and, at the age of 18 months, their levels in *Ucp2*$^{-/-}$ mice were significantly higher than in age-matched wild-type mice ($p < 0.0001$, two-way ANOVA, Fig. 4F).

3.5. *Ucp2*$^{-/-}$ mice have significantly lower body weight throughout their life than wild-type mice

Ucp2$^{-/-}$ mice and WT mice were weighed at the ages of 3, 6, 12, 18, and 24 months. *Ucp2*$^{-/-}$ mice had significantly less body weight than sex/age-matched wild-type mice at every tested age, except 3 month old females whose difference did not reach statistical significance but showed the same trend (Fig. 5, Supplementary Table 1).

Altogether, the body weight of male *Ucp2*$^{-/-}$ mice was reduced by 4.6% at 3 months, 6.1% at 6 months, 6.8% at 12 months, 11.0% at 18 months, and 4.8% at 24 months in comparison to wild-type mice. In females, the body weight of *Ucp2*$^{-/-}$ was reduced by 0.02% at 3 months, 4.4% at 6 months, 7.7% at 12 months, 9.2% at 18 months, and 13.3% at 24 months compared to age-matched wild-type mice.

3.6. Aged *Ucp2*$^{-/-}$ mice demonstrated distinct metabolic phenotypes

The metabolic phenotypes of *Ucp2*$^{-/-}$ and WT mice at ages of 3, 12, and 18 months were assessed using indirect calorimetry. This revealed that the respiratory exchange ratio (RER) during the resting period, i.e., at day time, is significantly affected by aging in both wild-type and *Ucp2*$^{-/-}$ mice (Fig. 6A, $p < 0.0001$, respectively, two-way ANOVA). In *Ucp2*$^{-/-}$ mice, the RER was significantly higher in 18 months old mice than in 3 months old ones (Supplementary Fig. 3A). The age difference in the RER was not observed during the active period, i.e., at night time, in *Ucp2*$^{-/-}$ mice, but in wild-type mice (Supplementary Fig. 3A, $p < 0.0001$, two-way ANOVA). There was a strain difference in RER at night time (Fig. 6B, $p = 0.0492$, two-way ANOVA), suggesting higher glucose use as energy source in *Ucp2*$^{-/-}$, whereas no difference was observed during the resting period (Fig. 6A). The energy expenditure (EE) during both the resting and the active periods was significantly affected by aging in both wild-type and *Ucp2*$^{-/-}$ mice ($p = 0.0091$ for resting EE in wild-type mice and $p < 0.0001$ *for the rests*, respectively, two-way ANOVA) (Fig. 6B). At 18 months of age, EE in both the resting and the active periods was significantly higher in *Ucp2*$^{-/-}$ mice than in wild-type mice (Fig. 6C and D). Voluntary exercise, recorded by InfraRed sensor in the calorimetric cages, demonstrated age-dependent reduction of the activity in *Ucp2*$^{-/-}$ mice in particular at night time ($p < 0.0001$, two-way ANOVA, Fig. 6C). At the age of 18 months, night time activities of *Ucp2*$^{-/-}$ mice were significantly less than those of age-matched wild-type mice (Fig. 6E, $p < 0.05$, two-way ANOVA). Thus, despite the reduced activities, EE is higher in aged *Ucp2*$^{-/-}$ mice. The levels of food and water intake were the same for *Ucp2*$^{-/-}$ and wild-type mice (data not shown).

3.7. Mitochondrial superoxide levels in brain were different between *Ucp2*$^{-/-}$ mice and wild-type mice

To assess the impact of the *Ucp2* gene on the mitochondrial function in aging, mitochondrial superoxide levels were measured in living brain slices in *Ucp2*$^{-/-}$ mice and wild-type mice at different ages, i.e. 3, 6, 12 and 24 months old (Fig. 7, Supplementary Fig. 4).

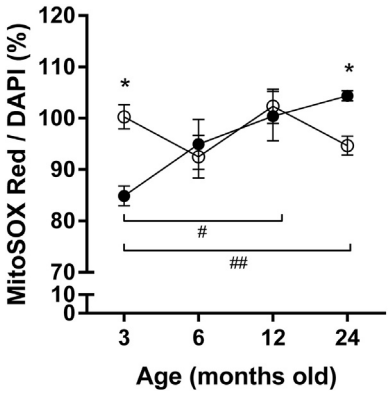

Fig. 7. Age-alteration of mitochondrial superoxide levels in brain tissue were evaluated in *Ucp2*$^{-/-}$ and wild-type mice. At 3 months of age the levels of mitochondrial superoxide in brain was significantly higher in *Ucp2*$^{-/-}$ mice ($^{*}p < 0.05$, *t*-test), while those at 24 months old were higher in wild-type mice than *Ucp2*$^{-/-}$ mice ($^{*}p < 0.05$, *t*-test). Within wild-type mice, the age-related increase of mitochondrial superoxide was observed ($^{\#}p < 0.05$, 3 months vs 12 months; $^{\#\#}p < 0.01$, 3 months vs 24 months). All values are presented as mean ± SEM.

An age-associated increase of mitochondrial superoxide was observed in wild-type mice. The mitochondrial superoxide in *Ucp2*$^{-/-}$ brain was significantly higher than wild-type mice at the age of 3 months, and remained at these higher levels throughout their life.

4. Discussion

In this study, we have demonstrated, using a large cohort of mice, that *Ucp2*$^{-/-}$ mice have a significantly shorter lifespan than sex-matched wild-type mice. In parallel, levels of circulating IGF-1 are higher in *Ucp2*$^{-/-}$ mice than in wild-type mice.

Andrews & Horvath previously also described the shorter lifespan of *Ucp2*$^{-/-}$ mice and proposed that it is due to increased ROS levels with the level of superoxide dismutase-2, a major antioxidant defense mechanism, reduced in these mice (Andrews and Horvath, 2009). Indeed, we and others also previously found *Ucp2*$^{-/-}$ mice to exhibit increased ROS production, which contributes to increased susceptibility to experimental autoimmune encephalomyelitis (Vogler et al., 2006) and to resistance to *Toxoplasma* infections (Arsenijevic et al., 2000) in these mice. In line with these previous findings, our results showed the higher levels of mitochondrial ROS in brain in *Ucp2*$^{-/-}$ mice than wild-type mice at the age of 3 months, and maintained high levels throughout their life. In contrast, wild-type mice brain demonstrated significantly lower levels of mitochondrial ROS than *Ucp2*$^{-/-}$, followed by age-associated increase. This finding indicates that the higher oxidative stress caused by the deficiency of *Ucp2* might have promoted aging phenotype at earlier age in *Ucp2*$^{-/-}$ mice, which could support the free radical theory of aging. Neuronal UCP2 are known to play critical roles in neuroprotection and health (Varela et al., 2016; Andrews et al., 2008; Fang et al., 2014), as well as lifespan (Conti et al., 2006; Fridell et al., 2005).

Furthermore, we have now highlighted suppression of the classical aging-related insulin/IGF-1 signaling (IIS) pathway by *Ucp2* as another major molecular mechanism for UCP-mediated lifespan extension. The IIS pathway is the most conserved aging-controlling pathway and regulates Forkhead box O (FOXO) family of transcription factors and the mammalian target of rapamycin (mTOR) complexes (López-Otín et al., 2013; Kenyon, 2010). Heterozygous mutant mice in the IGF-1 receptor gene (*Igf1r*$^{+/-}$) and mice deficient in the insulin receptor substrate 1 gene (*Irs1*$^{-/-}$) were long-lived (Holzenberger et al., 2003; Selman et al., 2008), while insulin receptor substrate 2 null mice (*Irs2*$^{-/-}$) were short-lived (Selman et al., 2008). A functionally relevant crosstalk between UCP2 and the IIS pathway was previously described in the context of insulin sensitivity of adipose tissue in rats, where the inhibition of *Ucp2* expression by antisense oligonucleotide technology improved insulin signal transduction (i.e. increase in insulin-induced tyrosine phosphorylation of the IR and IRS1, and a significant increase in serine phosphorylation of AKT and FOXO1) (De Souza et al., 2007).

In the present study, we have also found the incidence and time of onset of spontaneous ulcerative dermatitis (UD), a prototypical age-associated inflammatory disease, to depend on UCP2 signaling. Intriguingly, mice lacking the Insulin receptor substrate 1 gene (*Irs1*), a component of the major nutrient-sensing IIS pathway, are completely protected from UD, pointing at a critical role of the *Irs1*-mediated IIS pathway in UD pathogenesis (Selman et al., 2008). Hence, the increased susceptibility to UD in *Ucp2*$^{-/-}$ mice may be mechanistically due to the disinhibition of the IIS pathway in these mice.

Independent of UCP2 actions, *C57BL/6* mice develop an aging phenotype in peripheral blood defined by increased white blood cell counts with higher levels of neutrophils and reduced levels of lymphocytes with reduced levels of naive T cells and increased levels of memory T cells and NKT cells, as previously reported and publicly available at the Jackson Laboratory Mouse Phenome Database (Miller et al., 1997; Faunce et al., 2005; Grubb et al., 2014). However, this common aging phenotype was more pronounced in *Ucp2*$^{-/-}$ mice, specifically in respect to neutrophil and lymphocyte counts as well as, remarkably, to NKT cell counts. Taken together, this immune phenotype of *Ucp2*$^{-/-}$ mice as well as their enhanced susceptibility to UD indicate a counterregulatory role of *Ucp2* against "inflammaging", i.e., the age-related increase of inflammation in humans and mice (Franceschi et al., 2007). Accelerated inflammaging may also significantly contribute to the shorter life-span of *Ucp2*$^{-/}$ mice and its mechanisms will be further elucidated in future studies.

We have observed a significantly lower body weight in male and female *Ucp2*$^{-/-}$ mice starting only after the age of 3 months. In line with our results, previous studies reported no difference in body weight between 6- and 8-week-old wild-type and *Ucp2*$^{-/-}$ mice, but never examined weight of older mice (Arsenijevic et al., 2000; Zhang et al., 2001; De Souza et al., 2007). In both humans and mice, body weight gradually declines with age (Haines et al., 2001), the lower body weight of *Ucp2*$^{-/-}$ mice can, therefore, be considered another aspect of the premature-aging phenotype in these mice. A significant role of *Ucp2* in the regulation of body weight is further supported by the fact that *UCP2* mRNA levels in white adipose tissue and the body mass index are positively correlated in humans (Millet et al., 1997).

The smaller body size of *Ucp2*$^{-/-}$ mice is also reflected in our respiratory exchange ratio (RER) results: mice utilize body fat when they are resting (value closer to 0.7), whereas they use glucose as energy source (value closer to 1.0) when having access to standard food. RER, particularly during the night time, was significantly decreased with age in wild-type mice, which is consistent with a previously reported finding (Houtkooper et al., 2011). Despite comparable food and water intake, *Ucp2*$^{-/-}$ mice showed significantly higher RER levels during the night time, indicating that the *Ucp2*$^{-/-}$ mice use more glucose as energy source than age-matched wild-type mice. These results suggest that *Ucp2*$^{-/-}$ mice had less body fat available to burn than wild-type mice and, for this reason, resorted to glucose. Energy expenditure (lean mass heat production; EE) in wild-type mice showed an age-related reduction, while in *Ucp2*$^{-/-}$ mice EE remained high. By the age of 18 months, EE in wild-type mice had become significantly lower than that in *Ucp2*$^{-/-}$ mice. As a reduced rate of EE is reportedly a risk factor for body weight gain in humans (Ravussin et al., 1988), the higher EE in *Ucp2*$^{-/-}$ mice at the later stage of life may be also responsible for their reduced body weight. Moreover, in humans higher energy expenditure indicates higher energy turnover, which accelerates aging (Jumpertz et al., 2011). As a corollary, the higher energy turnover in *Ucp2*$^{-/-}$ may drive premature aging. In addition, a premature-aging model (*PolgA*$^{mut/mut}$ mtDNA mutator mice) that is deficient in *Ucp2* demonstrated the increased EE, which supports our finding (Kukat et al., 2014).

UCP2 is significantly increased in aged rats on the protein levels (Amaral et al., 2008) and, in the aforementioned premature aging mouse model, on both the mRNA and protein levels especially of cardiac tissue (Kukat et al., 2014). Furthermore, we and others have demonstrated that aged mice gain body weight (Houtkooper et al., 2011), and that *Ucp2* mRNA and protein expression are significantly higher in mouse models of spontaneous obesity (Zhang et al., 2001). These lines of evidence suggest that the physiological purpose of the increase in UCP2 levels in aging may be to adapt to increased fatty acid biosynthesis and consequently elevated lipid levels in aged individuals. Thus, mice deficient in *Ucp2* fail to adequately adapt to these age-related metabolic changes, which in turn shortens their lifespan. Furthermore, increased mRNA expression of *Ucp2* increase levels of free fatty acids (FFAs) (Samec et al., 1998). With FFAs and IGF-1 both suppressing growth hormone secretion from the hypothalamic-pituitary axis by a negative feedback-loop, which, as a result, also downregulates IGF-1 production in liver (Møller et al., 2009), it appears plausible that the higher levels of circulating IGF-1 in *Ucp2*$^{-/-}$ mice emerge from a defect of this negative feedback loop.

In summary, our study highlights a significant counterregulatory role of *Ucp2* against aging and age-related disease in mice. The protraction of aging is herein implemented by modulation of the insulin/IGF-1 signaling pathway through decreased blood levels of IGF-1, in addition

to the increased oxidative damage. These findings suggest that a targeted increase of *Ucp2* levels may prolong life in mammals.

Supplementary data to this article can be found online at http://dx.doi.org/10.1016/j.mito.2016.06.004.

Conflict of interest

Authors have no conflict of interests.

Acknowledgements

The authors thank Miriam Daumann, Miriam Freitag, Ann-Kathrin Brethack, and Ines Stölting for excellent technical support. This work was supported by grants from the Bundesministerium für Bildung und Forschung (BMBF, 0315892B and 0315892A) and the University of Lübeck (P01-2012).

References

Amaral, S., Mota, P., Rodrigues, A.S., Martins, L., Oliveira, P.J., Ramalho-Santos, J., 2008. Testicular aging involves mitochondrial dysfunction as well as an increase in UCP2 levels and proton leak. FEBS Lett. 582, 4191–4196.

Andrews, Z.B., Horvath, T.L., 2009. Uncoupling protein-2 regulates lifespan in mice. Am. J. Physiol. Endocrinol. Metab. 296, E621–E627.

Andrews, Z.B., Liu, Z.-W., Walllingford, N., Erion, D.M., Borok, E., Friedman, J.M., Tschöp, M.H., Shanabrough, M., Cline, G., Shulman, G.I., Coppola, A., Gao, X.-B., Horvath, T.L., Diano, S., 2008. UCP2 mediates ghrelin's action on NPY/AgRP neurons by lowering free radicals. Nature 454, 846–851.

Arsenijevic, D., Onuma, H., Pecqueur, C., Raimbault, S., Manning, B.S., Miroux, B., Couplan, E., Alves-Guerra, M.-C., Goubern, M., Surwit, R., Bouillaud, F., Richard, D., Collins, S., Ricquier, D., 2000. Disruption of the uncoupling protein-2 gene in mice reveals a role in immunity and reactive oxygen species production. Nat. Genet. 26, 435–439.

Barbieri, M., Boccardi, V., Esposito, A., Papa, M., Vestini, F., Rizzo, M.R., Paolisso, G., 2012. A/ASP/VAL allele combination of IGF1R, IRS2, and UCP2 genes is associated with better metabolic profile, preserved energy expenditure parameters, and low mortality rate in longevity. Age (Dordr.) 34, 235–245.

Bouillaud, F., 2009. UCP2, not a physiologically relevant uncoupler but a glucose sparing switch impacting ROS production and glucose sensing. Biochim. Biophys. Acta 1787, 377–383.

Conti, B., Sanchez-Alavez, M., Winsky-Sommerer, R., Morale, M.C., Lucero, J., Brownell, S., Fabre, V., Huitron-Resendiz, S., Henriksen, S., Zorrilla, E.P., de Lecea, L., Bartfai, T., 2006. Transgenic mice with a reduced core body temperature have an increased life span. Science 314, 825–828.

De Souza, C.T., Araújo, E.P., Stoppiglia, L.F., Pauli, J.R., Ropelle, E., Rocco, S.A., Marin, R.M., Franchini, K.G., Carvalheira, J.B., Saad, M.J., Boschero, A.C., Carneiro, E.M., Velloso, L.A., 2007. Inhibition of UCP2 expression reverses diet-induced diabetes mellitus by effects on both insulin secretion and action. FASEB J. 21, 1153–1163.

Emre, Y., Hurtaud, C., Nübel, T., Criscuolo, F., Ricquier, D., Cassard-Doulcier, A.-M., 2007. Mitochondria contribute to LPS-induced MAPK activation via uncoupling protein UCP2 in macrophages. Biochem. J. 402, 271–278.

Fang, E.F., Scheibye-Knudsen, M., Brace, L.E., Kassahun, H., SenGupta, T., Nilsen, H., Mitchell, J.R., Croteau, D.L., Bohr, V.A., 2014. Defective mitophagy in XPA via PARP-1 hyperactivation and NAD(+)/SIRT1 reduction. Cell 157, 882–896.

Faul, F., Erdfelder, E., Lang, A.-G., Buchner, A., 2007. G*Power 3: a flexible statistical power analysis program for the social, behavioral, and biomedical sciences. Behav. Res. Methods 39, 175–191.

Faunce, D.E., Palmer, J.L., Paskowicz, K.K., Witte, P.L., Kovacs, E.J., 2005. CD1d-restricted NKT cells contribute to the age-associated decline of T cell immunity. J. Immunol. 175, 3102–3109.

Fleury, C., Neverova, M., Collins, S., Raimbault, S., Champigny, O., Levi-Meyrueis, C., Bouillaud, F., Seldin, M.F., Surwit, R.S., Ricquier, D., Warden, C.H., 1997. Uncoupling protein-2: a novel gene linked to obesity and hyperinsulinemia. Nat. Genet. 15, 269–272.

Franceschi, C., Capri, M., Monti, D., Giunta, S., Olivieri, F., Sevini, F., Panourgia, M.P., Invidia, L., Celani, L., Scurti, M., Cevenini, E., Castellani, G.C., Salvioli, S., 2007. Inflammaging and anti-inflammaging: a systemic perspective on aging and longevity emerged from studies in humans. Mech. Ageing Dev. 128, 92–105.

Fridell, Y.-W.C., Sánchez-Blanco, A., Silvia, B.A., Helfand, S.L., 2005. Targeted expression of the human uncoupling protein 2 (hUCP2) to adult neurons extends life span in the fly. Cell Metab. 1, 145–152.

Grubb, S.C., Bult, C.J., Bogue, M.A., 2014. Mouse phenome database. Nucleic Acids Res. 42, D825–D834.

Haines, D.C., Chattopadhyay, S., Ward, J.M., 2001. Pathology of aging B6;129 mice. Toxicol. Pathol. 29, 653–661.

Holzenberger, M., Dupont, J., Ducos, B., Leneuve, P., Géloën, A., Even, P.C., Cervera, P., Le Bouc, Y., 2003. IGF-1 receptor regulates lifespan and resistance to oxidative stress in mice. Nature 421, 182–187.

Houtkooper, R.H., Argmann, C., Houten, S.M., Cantó, C., Jeninga, E.H., Andreux, P.A., Thomas, C., Doenlen, R., Schoonjans, K., Auwerx, J., 2011. The metabolic footprint of aging in mice. Sci. Rep. 1, 134.

Jumpertz, R., Hanson, R.L., Sievers, M.L., Bennett, P.H., Nelson, R.G., Krakoff, J., 2011. Higher energy expenditure in humans predicts natural mortality. J. Clin. Endocrinol. Metab. 96, E972–E976.

Kastenmayer, R.J., Fain, M.A., Perdue, K.A., 2006. A retrospective study of idiopathic ulcerative dermatitis in mice with a C57BL/6 background. J. Am. Assoc. Lab. Anim. Sci. 45, 8–12.

Kenyon, C.J., 2010. The genetics of ageing. Nature 464, 504–512.

Krauss, S., Zhang, C.-Y., Lowell, B.B., 2002. A significant portion of mitochondrial proton leak in intact thymocytes depends on expression of UCP2. Proc. Natl. Acad. Sci. U. S. A. 99, 118–122.

Kukat, A., Dogan, S.A., Edgar, D., Mourier, A., Jacoby, C., Maiti, P., Mauer, J., Becker, C., Senft, K., Wibom, R., Kudin, A.P., Hultenby, K., Flögel, U., Rosenkranz, S., Ricquier, D., Kunz, W.S., Trifunovic, A., 2014. Loss of UCP2 attenuates mitochondrial dysfunction without altering ROS production and uncoupling activity. PLoS Genet. 10, e1004385.

López-Otín, C., Blasco, M.A., Partridge, L., Serrano, M., Kroemer, G., 2013. The hallmarks of aging. Cell 153, 1194–1217.

Mayer, J., Reichart, G., Tokay, T., Lange, F., Baltrusch, S., Junghanss, C., Wolkenhauer, O., Jaster, R., Kunz, M., Tiedge, M., Ibrahim, S., Fuellen, G., Köhling, R., 2015. Reduced adolescent-age spatial learning ability associated with elevated juvenile-age superoxide levels in complex I mouse mutants. PLoS One 10, e0123863.

Miller, R.A., Chrisp, C., Galecki, A., 1997. CD4 memory T cell levels predict life span in genetically heterogeneous mice. FASEB J. 11, 775–783.

Millet, L., Vidal, H., Andreelli, F., Larrouy, D., Riou, J.P., Ricquier, D., Laville, M., Langin, D., 1997. Increased uncoupling protein-2 and -3 mRNA expression during fasting in obese and lean humans. J. Clin. Invest. 100, 2665–2670.

Møller, N., Gormsen, L.C., Schmitz, O., Lund, S., Jørgensen, J.O.L., Jessen, N., 2009. Free fatty acids inhibit growth hormone/signal transducer and activator of transcription-5 signaling in human muscle: a potential feedback mechanism. J. Clin. Endocrinol. Metab. 94, 2204–2207.

Moon, J.-S., Lee, S., Park, M.-A., Siempos, I.I., Haslip, M., Lee, P.J., Yun, M., Kim, C.K., Howrylak, J., Ryter, S.W., Nakahira, K., Choi, A.M.K., 2015. UCP2-induced fatty acid synthase promotes NLRP3 inflammasome activation during sepsis. J. Clin. Invest. 125, 665–680.

Partridge, L., Gems, D., 2002. Mechanisms of ageing: public or private? Nat. Rev. Genet. 3, 165–175.

Pecqueur, C., Alves-Guerra, M.C., Gelly, C., Levi-Meyrueis, C., Couplan, E., Collins, S., Ricquier, D., Bouillaud, F., Miroux, B., 2001. Uncoupling protein 2, in vivo distribution, induction upon oxidative stress, and evidence for translational regulation. J. Biol. Chem. 276, 8705–8712.

Pecqueur, C., Bui, T., Gelly, C., Hauchard, J., Barbot, C., Bouillaud, F., Ricquier, D., Miroux, B., Thompson, C.B., 2008. Uncoupling protein-2 controls proliferation by promoting fatty acid oxidation and limiting glycolysis-derived pyruvate utilization. FASEB J. 22, 9–18.

Petkova, S.B., Yuan, R., Tsaih, S.-W., Schott, W., Roopenian, D.C., Paigen, B., 2008. Genetic influence on immune phenotype revealed strain-specific variations in peripheral blood lineages. Physiol. Genomics 34, 304–314.

Ravussin, E., Lillioja, S., Knowler, W.C., Christin, L., Freymond, D., Abbott, W.G., Boyce, V., Howard, B.V., Bogardus, C., 1988. Reduced rate of energy expenditure as a risk factor for body-weight gain. N. Engl. J. Med. 318, 467–472.

Riera, C.E., Dillin, A., 2015. Tipping the metabolic scales towards increased longevity in mammals. Nat. Cell Biol. 17, 196–203.

Ristow, M., 2014. Unraveling the truth about antioxidants: mitohormesis explains ROS-induced health benefits. Nat. Med. 20, 709–711.

Rose, G., Crocco, P., De Rango, F., Montesanto, A., Passarino, G., 2011. Further support to the uncoupling-to-survive theory: the genetic variation of human UCP genes is associated with longevity. PLoS One 6, e29650.

Rousset, S., Alves-Guerra, M.-C., Mozo, J., Miroux, B., Cassard-Doulcier, A.-M., Bouillaud, F., Ricquier, D., 2004. The biology of mitochondrial uncoupling proteins. Diabetes 53 (Suppl. 1), S130–S135.

Samec, S., Seydoux, J., Dulloo, A.G., 1998. Role of UCP homologues in skeletal muscles and brown adipose tissue: mediators of thermogenesis or regulators of lipids as fuel substrate? FASEB J. 12, 715–724.

Schulz, T.J., Zarse, K., Voigt, A., Urban, N., Birringer, M., Ristow, M., 2007. Glucose restriction extends *Caenorhabditis elegans* life span by inducing mitochondrial respiration and increasing oxidative stress. Cell Metab. 6, 280–293.

Selman, C., Lingard, S., Choudhury, A.I., Batterham, R.L., Claret, M., Clements, M., Ramadani, F., Okkenhaug, K., Schuster, E., Blanc, E., Piper, M.D., Al-Qassab, H., Speakman, J.R., Carmignac, D., Robinson, I.C.A., Thornton, J.M., Gems, D., Partridge, L., Withers, D.J., 2008. Evidence for lifespan extension and delayed age-related biomarkers in insulin receptor substrate 1 null mice. FASEB J. 22, 807–818.

Tapia, P.C., 2006. Sublethal mitochondrial stress with an attendant stoichiometric augmentation of reactive oxygen species may precipitate many of the beneficial alterations in cellular physiology produced by caloric restriction, intermittent fasting, exercise and dietary phytonutrients: "mitohormesis" for health and vitality. Med. Hypotheses 66, 832–843.

Varela, L., Schwartz, M.L., Horvath, T.L., 2016. Mitochondria controlled by UCP2 determine hypoxia-induced synaptic remodeling in the cortex and hippocampus. Neurobiol. Dis. 90, 68–74.

Vogler, S., Pahnke, J., Rousset, S., Ricquier, D., Moch, H., Miroux, B., Ibrahim, S.M., 2006. Uncoupling protein 2 has protective function during experimental autoimmune encephalomyelitis. Am. J. Pathol. 168, 1570–1575.

Vozza, A., Parisi, G., De Leonardis, F., Lasorsa, F.M., Castegna, A., Amorese, D., Marmo, R., Calcagnile, V.M., Palmieri, L., Ricquier, D., Paradies, E., Scarcia, P., Palmieri, F., Bouillaud, F., Fiermonte, G., 2014. UCP2 transports C4 metabolites out of mitochondria, regulating glucose and glutamine oxidation. Proc. Natl. Acad. Sci. U. S. A. 111, 960–965.

Weir, J.B.D.B., 1949. New methods for calculating metabolic rate with special reference to protein metabolism. J. Physiol. Lond. 109, 1–9.
Williams, L.K., Csaki, L.S., Cantor, R.M., Reue, K., Lawson, G.W., 2012. Ulcerative dermatitis in C57BL/6 mice exhibits an oxidative stress response consistent with normal wound healing. Comp. Med. 62, 166–171.
Yuan, R., Tsaih, S.-W., Petkova, S.B., Marin de Evsikova, C., Xing, S., Marion, M.A., Bogue, M.A., Mills, K.D., Peters, L.L., Bult, C.J., Rosen, C.J., Sundberg, J.P., Harrison, D.E., Churchill, G.A., Paigen, B., 2009. Aging in inbred strains of mice: study design and interim report on median lifespans and circulating IGF1 levels. Aging Cell 8, 277–287.
Yuan, R., Meng, Q., Nautiyal, J., Flurkey, K., Tsaih, S.-W., Krier, R., Parker, M.G., Harrison, D.E., Paigen, B., 2012. Genetic coregulation of age of female sexual maturation and lifespan through circulating IGF1 among inbred mouse strains. Proc. Natl. Acad. Sci. U. S. A. 109, 8224–8229.
Zhang, C.Y., Baffy, G., Perret, P., Krauss, S., Peroni, O., Grujic, D., Hagen, T., Vidal-Puig, A.J., Boss, O., Kim, Y.B., Zheng, X.X., Wheeler, M.B., Shulman, G.I., Chan, C.B., Lowell, B.B., 2001. Uncoupling protein-2 negatively regulates insulin secretion and is a major link between obesity, beta cell dysfunction, and type 2 diabetes. Cell 105, 745–755.